Environ. Sci. Technol. **2006**, *40,* 4174−4180

Complexation of Mercury(II) in Soil Organic Matter: EXAFS Evidence for Linear Two-Coordination with Reduced Sulfur Groups

ULF SKYLLBERG,*,† PAUL R. BLOOM,‡ JIN QIAN,† CHUNG-MIN LIN,‡ AND WILLIAM F. BLEAM§

Department of Forest Ecology, Swedish University of Agricultural Sciences, S-901 83 Umeå, Sweden, Department of Soil, Water and Climate, University of Minnesota, St. Paul, Minnesota 55108, and Department of Soil Science, University of Wisconsin, Madison, Wisconsin 53706

The chemical speciation of inorganic mercury (Hg) is to a great extent controlling biologically mediated processes, such as mercury methylation, in soils, sediments, and surface waters. Of utmost importance are complexation reactions with functional groups of natural organic matter (NOM), indirectly determining concentrations of bioavailable, inorganic Hg species. Two previous extended X-ray absorption fine structure (EXAFS) spectroscopic studies have revealed that reduced organic sulfur (S) and oxygen/nitrogen (O/N) groups are involved in the complexation of Hg(II) to humic substances extracted from organic soils. In this work, covering intact organic soils and extending to much lower concentrations of Hg than before, we show that Hg is complexed by two reduced organic S groups (likely thiols) at a distance of 2.33 Å in a linear configuration. Furthermore, a third reduced S (likely an organic sulfide) was indicated to contribute with a weaker second shell attraction at a distance of 2.92−3.08 Å. When all high-affinity S sites, corresponding to 20−30% of total reduced organic S, were saturated, a structure involving one carbonyl-O or amino-N at 2.07 Å and one carboxyl-O at 2.84 Å in the first shell, and two second shell C atoms at an average distance of 3.14 Å, gave the best fit to data. Similar results were obtained for humic acid extracted from an organic wetland soil. We conclude that models that are in current use to describe the biogeochemistry of mercury and to calculate thermodynamic processes need to include a two-coordinated complexation of Hg(II) to reduced organic sulfur groups in NOM in soils and waters.

Introduction

Mercury (Hg) is one of the most toxic elements known to man. As a consequence of fossil fuel combustion and long-range transport of emitted Hg in the atmosphere, northern latitudes are subjected to a large-scale contamination of soils and waters. A major concern is the transformation of inorganic Hg to methylmercury (MeHg) in wetlands (*1*), along hydrological pathways in soils (*2*), and in surface waters (*3*), which has led to highly elevated concentrations in fish (*4*). The buildup of MeHg in soils and sediments is a net result of methylation and demethylation processes. There is a consensus that the methylation process is biologically mediated, mainly by sulfate-reducing bacteria (SRB), whereas demethylation is believed to occur as both abiotic and biotic reactions (*5*). Laboratory experiments strongly indicate the importance of dissolved, neutral inorganic Hg species, such as $HgCl_2^0$, $Hg(SH)_2^0$, and HgS^0, as the main forms available for uptake by SRB (*6*, *7*). Based on these results, and on determined values of log K_{OC} for the complexation of Hg to natural organic matter (NOM) on the order of $10^{25}-10^{30}$ (*8*−*10*), we conclude that the complexation of Hg to NOM functional groups in many terrestrial and aquatic environments controls the concentration of small inorganic Hg molecules bioavailable for methylating bacteria. To improve our understanding and models used to predict solubility, net methylation rates, and biouptake of Hg/MeHg, more detailed information is needed about the strength and structure of these Hg−NOM complexes at low Hg concentrations.

Two extended X-ray absorption fine structure (EXAFS) spectroscopic studies have been reported on the association between Hg and extracted humic substances from organic wetland soils (*11*, *12*). In both studies reduced S groups were shown to be increasingly involved in the complexation with decreased concentrations of Hg. However, in both studies additions of Hg exceeded the concentration of high-affinity reduced S sites in the samples, and supposedly weaker O/N ligands were involved in the complexation as well. Calculations based on the sample with the lowest Hg concentrations in the study by Hesterberg and co-workers (*12*; having a molar ratio of Hg to reduced organic S of 0.26) suggested that 70% of Hg was complexed by two reduced S groups. Because of a relatively low signal-to-noise ratio, second coordination shell data could not be resolved to reveal the kind of reduced S groups involved (thiols, sulfides, disulfides). In the study by Xia et al. (*11*), data for first and second shell contributions could be equally well fitted by a model with one thiol and one O/N group or by one disulfide and one O/N group. The molar ratio between Hg and reduced organic S was 3.1, and therefore data were most likely not reflecting the strongest coordination found under natural conditions. To our knowledge, there are no reported EXAFS studies on the Hg bonding to intact soils.

The aim of this study was to determine the coordination chemistry of Hg in intact organic soils and to extend the ratio of Hg to reduced organic S to the lowest value possible in order to approach the situation in soil environments. Thus, EXAFS experiments were conducted with intact (freeze-dried) organic soils at Hg additions between 0.1 and 4.0 mg of Hg g^{-1}, corresponding to a Hg to reduced organic S molar ratio of 0.01−0.33. In addition, humic acid extracted from an organic wetland soil, very similar to the one used by Xia et al. (*11*), was investigated at a Hg to reduced organic S molar ratio of 0.23−8.0.

Materials and Methods

Organic Soil, Humic Acids, and Model Compounds. An organic peat soil typical for the discharge area of a boreal forest catchment in northern Sweden (Nyänget catchment, Svartberget Research Station, 64° 14′ N, 19° 46′ E) was used in this study. The soil was sampled at 10−20 cm depth, 10

---

* Corresponding author phone: +46 (0) 090-786 84 60; fax: +46 (0) 090-786 81 63; e-mail: ulf.skyllberg@sek.slu.se.

† Swedish University of Agricultural Sciences.

‡ University of Minnesota.

§ University of Wisconsin.

10.1021/es0600577 CCC: $33.50

cm above the groundwater table and 2 m from a small draining stream. In Skyllberg et al. (*2*) a more detailed description of the soil (referred to as soil 6) and the site is presented. Mercury nitrate, dissolved in a minimum of double-distilled water, was added to soil samples to yield 0.1, 0.6, 1.2, 3.0, and 4.0 mg of Hg g^{-1} (dry mass of soil). High-viscosity suspensions were mixed continuously for 7 days to reach equilibrium. The pH was in the range 3.8−4.0 for all samples. Samples were then freeze-dried and pellets were prepared 1−2 h before each EXAFS experiment.

Humic acids (HA) were extracted from the upper 10 cm of an organic soil in the discharge area at the edge of a boreal fen (watershed S3) in the Marcell Experimental Forest, north of Grand Rapids in northern Minnesota. The extraction procedure followed the method recommended by the International Humic Substance Society (*13*). Mercury was added to HA suspensions as $Hg(NO_3)_2$. After 24 h of equilibration on a reciprocal shaker, suspensions were centrifuged and the flocculated HA was freeze-dried. The pH was between 3 and 3.5. Actual Hg contents of HA were determined by cold vapor fluorescence atomic spectroscopy, yielding 3.2, 6.2, 14, 60, and 128 mg of Hg g^{-1} (dry mass of HA). Freeze-dried organic soil and HA samples were mounted in 2-mm-thick acrylic holders sealed with 2.5 μm Kapton tape (Furon, CHR) windows prior to EXAFS analyses.

Total concentrations of C, N, and S were 493, 18.3, and 4.1 mg g^{-1}, respectively, in the organic soil and 531, 29.6, and 4.3 mg g^{-1}, respectively, in the HA, as determined by a CHN analyzer (Perkin-Elmer, 2400 CHN) and a LECO analyzer (LECO Corp., St. Joseph, MI). The ash content was 4% in the organic soil and 0.2% in the HA. The concentration of reduced organic S (Org-S_{RED}) was determined in accordance with Xia et al. (*14*) as the sum of S electronic oxidation states of 0.2 and 0.9−1.0, using K-edge sulfur XANES at beamline X19A at NSLS, Brookhaven, NY. The S XANES spectrum and fit for the organic soil is illustrated in ref *15*. In the organic soil, Org-S_{RED} was 61% of total S, and in HA Org-S_{RED} was 51% of total S. Thus, additions of Hg resulted in molar Hg (II)/Org-S_{RED} ratios of 0.01, 0.05, 0.10, 0.25, and 0.33 in the organic soil and 0.23, 0.40, 0.88, 3.8, and 8.0 in HA.

As model compounds, cation-exchange resins with carboxyl (RCOOH) and thiol (RSH) groups were used. Thiol resins with inorganic mercury (Hg−SR) and methylmercury (MeHg−SR) were prepared by equilibrating a Duolite GT73 resin (Rohm and Hass) with HgOH and MeHgOH solution, yielding a concentration of 2.5 mg of Hg g^{-1} on a dry mass basis of the resin. This corresponds to 0.3% saturation of thiol groups by Hg^{2+} and $MeHg^{+}$. A carboxylic resin (200−400 mesh Bio-Rex 70) was used to prepare a MeHg−OOCR model in the same way, yielding 2.5 mg of Hg g^{-1}. This corresponds to 0.1% saturation of carboxyl groups by $MeHg^{+}$. After 24 h of equilibration, the resins were washed with distilled water three times. All resins were freeze-dried, ground, mixed with boron nitride, pressed to pellets, and finally mounted in 2-mm-thick acrylic holders sealed with 2.5 μm Kapton tape (Furon, CHR) windows. In addition, red HgS (Merck) was prepared as a standard without any further preparation than grinding, diluting with boron nitride, and pressing to a thin pellet.

Hg L_{III}-Edge EXAFS Data Collection and Analyses. All organic soil samples, the HA samples with 3.2 and 6.2 mg of Hg g^{-1}, and the MeHg resins were analyzed on the undulator beamline ID26 at the European Synchrotron Radiation Facility (ESRF, Grenoble, France). The HA samples with addtitions of 14, 60, and 128 mg of Hg g^{-1} and the Hg−thiol resin were analyzed on the bending-magnet beamline X10C at the National Synchrotron Light Source (NSLS, Brookhaven National Laboratory, Upton, NY). Machine conditions and setup are described in the Supporting Information. Standard EXAFS data reduction procedures were undertaken using the program WinXAS (*17*), as detailed in the Supporting Information.

Theoretical EXAFS scattering curves and parameters were generated by the FEFF-7 computer program (*18*, *19*). Theoretical structural parameters for Hg−S, Hg−O, and Hg−C associations reported from well-defined organic molecules (Table S1, Supporting Information) were used as input for FEFF calculations. For the crystalline model compound cinnabar (α-HgS, red) the coordination number (CN) was fixed at 2.0, based on its theoretical structure, and the amplitude reduction factor (S_0^2) was determined to be 0.90. When the CN was fixed at 2.0 for the sum of first shell atoms in MeHg−OOCR, MeHg−SR, and Hg−SR resin model compounds, the determined S_0^2 was 0.90, 0.93, and 0.90, respectively. Therefore S_0^2 was fixed at 0.90 in the final fits of all model compounds, organic soil, and HA samples. To keep the maximum number of floating parameters less than the number of statistically independent data points (calculated as $N_{idp} = 2\Delta k\Delta R/\pi$ and presented in Table S2, Supporting Information), the following parameters were fixed or constrained during final fitting: (1) first shell coordination numbers of C and O/N atoms were fixed at 1.0 for MeHg−OOCR and MeHg−SR model compounds, (2) for model compounds, organic soil, and HA samples containing S atoms, the CN of first shell S and CN of second shell distant C (assumed bound to S) were correlated and set equal, and (3) the Debye−Waller factor (σ^2) was fixed at 0.002 Å^2 for all second and higher shell contributions. This relatively small value on σ^2 for higher shells was justified by the Hg−S resin ($\sigma^2 = 0.002$ Å^2 for second shell C). Data on methylmercury complexation to humic substances were best fitted with $\sigma^2 = 0.003-0.004$ Å^2 in second and third atomic shells (*20*). The shift of the edge energy, ΔE_0, was allowed to float but constrained to be equal for atomic shells.

Complexation Models. In Table S1 (Supporting Information), data on bond distances and bond angles are reported as ranges for well-defined organic molecules in which Hg^{2+} is associated to C, O, N, and S atoms in thiolates, amino acids, and carboxylates (*21*−*33*). These data were used to construct the following two-coordinated linear models in FEFF: C−S−Hg−S−C, C−S−Hg−O/N−C, and C−O/N−Hg−O/N−C. These models, given the constraints above, were all fitted to experimental data.

Results and Discussion

Model Compounds. In Figure 1 experimental data and fits are illustrated for model compounds, as well as for HA and organic soil samples. Methylmercury forms only one bond to thiol and carboxyl resins (*15*), which are therefore excellent reference compounds for first shell O/S and second shell Hg---O and Hg---C associations. The C−Hg distance in MeHg was determined to be 2.03−2.04 Å (Table 1), which is in agreement with C−Hg distances in well-defined organic molecules (*34*). This also holds for the Hg−O distance of 2.09 Å in the carboxyl resin and the Hg−S distance in the thiol resins of 2.33 Å (cf. Table S1, Supporting Information). The best fit to MeHg−OOCR data was obtained with 0.8 C and 0.8 O atoms at a distance of 2.90 and 2.77 Å from Hg in the second shell (Table 2), respectively. The second shell Hg---O distance is within the range, whereas the Hg---C distance is slightly longer than the reported range for carboxyls (Table S1, Supporting Information). It should be taken into consideration that the rigidity of the resin may result in longer second shell distances than in dissolved, more flexible organic molecules. In the thiol resins, a second shell of 0.7 C (MeHg−SR) and 1.5 C (Hg−SR) atoms was encountered at 3.29−3.32 Å, well in agreement with the range reported for low molecular weight thiols (Table S1, Supporting Information). It should be noted that the second shell C distance in general is substantially longer when Hg is complexed by a thiol group,

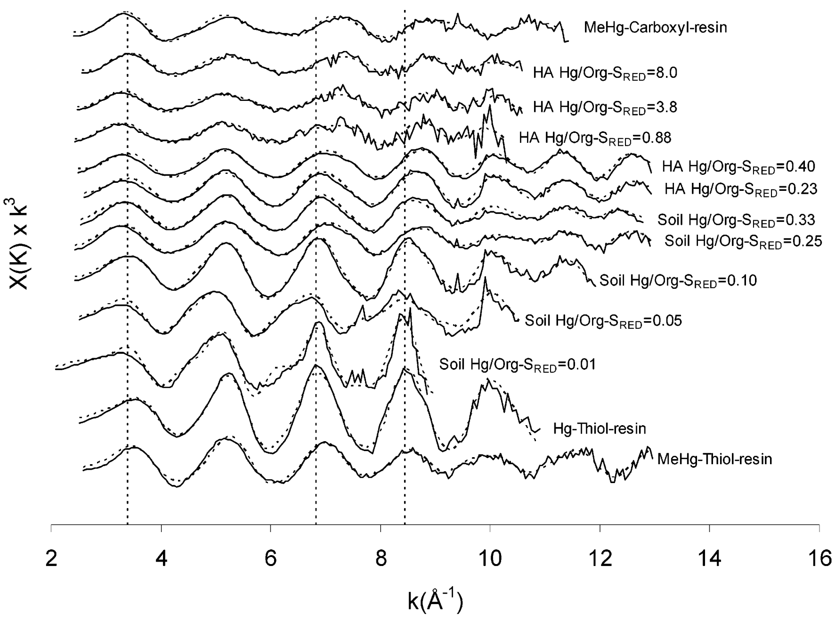

FIGURE 1. Experimental EXAFS data (solid lines) and fits (dotted lines) for model compounds, HA, and organic soil samples. Vertical dotted lines are inserted to facilitate comparison of frequencies.

TABLE 1. Least-Squares Fits of the First Coordination Shell for Resin Model Compounds (MeHg−OOCR, MeHg−SR, Hg−SR), Cinnabar (HgS), Humic Acid (HA), and Organic Soil Samples[a]

			1st C shell			1st O/N shell			1st S shell		
sample	Hg (mg g^{-1})	Hg/Org-S_{RED} (mol/mol)	CN	R (Å)	σ^2 (Å^2)	CN	R (Å)	σ^2 (Å^2)	CN	R (Å)	σ^2 (Å^2)
MeHg−OOCR			1.0[b]	2.03	0.006	1.0[b]	2.09	0.004			
MeHg−SR			1.0[b]	2.04	0.002				1.0[c]	2.33	0.003
Hg−SR									2.2[c]	2.33	0.003
HgS									2.0[b]	2.37	0.002
HA	128	8.0				1.5	2.06	0.010			
HA	60	3.8				1.5	2.06	0.010			
HA	14	0.88				1.7	2.08	0.010			
HA	6.2	0.40				1.0	2.05	0.004	0.7[c]	2.34	0.004
HA	3.2	0.23				0.9	2.07	0.004	1.0[c]	2.34	0.004
organic soil	4.0	0.33				0.9	2.06	0.004	0.8[c]	2.34	0.004
organic soil	3.0	0.25				1.0	2.04	0.004	0.7[c]	2.32	0.004
organic soil	1.2	0.10				0.7	2.09	0.001	1.5[c]	2.36	0.004
organic soil	0.6	0.05							1.7[c]	2.33	0.008
organic soil	0.1	0.01							2.0[c]	2.33	0.005

[a] CN = coordination number; R = bond distance; σ^2 = Debye−Waller factor. The ΔE_0 and the goodness of fit are reported in Table 2. [b] Numbers were fixed during fitting. [c] CN was correlated (set equal) to CN of second shell C bound to S (cf. Table 2) during fitting.

as compared to a carboxyl group, due to the longer first shell distance of Hg−S. The second shell Hg---C distance is reported to be 3.35 Å in the $Hg(SC)_2$ core of proteins (*21*), whereas other studies have shown somewhat shorter distances in *S*-aryl compounds (3.14−3.20 Å; *23*) and in mercaptoacetic acid (3.20 Å; *22*).

In all resin model compounds, as well as in cinnabar HgS(s), the approximately 180° linear coordination (X−Hg−X, X = C, O, or S) gives rise to a multiple scattering (MS) along the four-legged path Hg → X → Hg → X → Hg. This MS contribution appears at a distance of 4.20 Å [approximately corresponding to the sum of 2.03 Å (C−Hg) and 2.09 Å (O−Hg)] in the MeHg−OOCR resin, at 4.40 Å [sum of 2.04 Å (C−Hg) and 2.33 Å (Hg−S)] in the MeHg−SR resin, and at 4.65 and 4.73 Å [2 times 2.33 Å (S−Hg−S)] in the Hg−SR resin and HgS(s), respectively. In the Hg−SR and MeHg−SR resins, a three-legged MS contribution at 3.54−3.64 Å (Hg → S → C → Hg) was included. The sum of three-legged and four-legged MS contributions improved the fits by approximately 10% in the MeHg−SR and Hg−SR resins. Illustrations of Fourier transform (FT) data and fits for MeHg−OOCR and MeHg−SR resin model compounds are included in Figure S1 (Supporting Information).

Organic Soil. Coordination numbers (CN) and distances determined in the organic soil samples with Hg/Org-S_{RED} ratios 0.01 and 0.05 show that Hg is complexed with two S atoms at 2.33 Å in the first coordination shell (Table 1). This association is reflected by the main peak at ~1.9 Å in the FT spectra (Figure 2).

Introduction of O/N atoms in the first shell significantly lowered the goodness of fit. The strong feature at ~3.9 Å in the radial structure functions (RSF) is due to the multiple scattering of the four-legged path Hg → S → Hg → S → Hg and is direct evidence for a linear configuration with two sulfur groups. The MS occurs at 2 times the distance to each of the S atoms (2 × 2.33 Å = 4.66 Å). The fact that the CN was 1.9 for the MS path for the Hg/Org-S_{RED} = 0.01 sample suggests that all Hg atoms are involved in an almost perfect, linear S−Hg−S configuration with close to a 180° bond angle. In the Hg/Org-S_{RED} = 0.05 sample the CN decreased to 0.8, suggesting that at higher Hg loading the linear coordination is distorted.

TABLE 2. Least-Squares Fits of Second and Higher Coordination Shells in Model Compounds, HA, and Organic Soil Samples

			2nd O shell			2nd C(−O/N) shell			2nd S shell			2nd C(−S) shell			multiple X−Hg−X				
sample	Hg (mg g^{-1})	Hg/S$_{RED}$ (mol/mol)	CN	R (Å)	σ^2 (Å^2)	CN	R (Å)	σ^2 (Å^2)	CN	R (Å)	σ^2 (Å^2)	CN	R (Å)	σ^2 (Å^2)	CN	R (Å)	σ^2 (Å^2)	ΔE_0	R_P[a] (%)
MeHg−OOCR			0.8[b]	2.77	0.002[d]	0.8[b]	2.90	0.002[d]							1.2	4.20	0.002[d]	6.0	19
MeHg−SR[e]												1.0[c]	3.32	0.005	1.0	4.40	0.002[d]	0.9	8.9
Hg−SR[e]												2.2[c]	3.29	0.002	1.0	4.64	0.002[d]	5.2	4.6
HgS															1.2	4.73	0.002[d]	4.7	4.5
HA	128	8.0	1.1	2.86	0.002[d]	1.5	3.14	0.002[d]										9.0	20
HA	60	3.8	1.1	2.85	0.002[d]	1.5	3.14	0.002[d]										9.2	25
HA	14	0.88	0.9	2.88	0.002[d]	2.0	3.21	0.002[d]										9.5	42
HA	6.2	0.40	1.0	2.81	0.002[d]	1.6	3.11	0.002[d]				0.7[c]	3.31	0.002[d]	0.2	4.73	0.002[d]	8.0	6.4
HA	3.2	0.23	0.9	2.81	0.002[d]	1.7	3.11	0.002[d]				1.0[c]	3.30	0.002[d]	0.2	4.66	0.002[d]	8.2	6.9
organic soil	4.0	0.33	0.7	2.87	0.002[d]	1.3	3.15	0.002[d]				0.8[c]	3.33	0.002[d]	0.3	4.66	0.002[d]	7.6	7.5
organic soil	3.0	0.25	1.0	2.83	0.002[d]	1.5	3.10	0.002[d]				0.7[c]	3.29	0.002[d]	0.3	4.67	0.002[d]	7.6	5.1
organic soil	1.2	0.10	0.8	2.84	0.002[d]	1.8	3.15	0.002[d]				1.5[c]	3.33	0.002[d]	0.8	4.64	0.002[d]	8.4	4.4
organic soil	0.6	0.05							0.5	2.92	0.002[d]	1.7[c]	3.42	0.002[d]	0.8	4.57	0.002[d]	−0.6	19
organic soil	0.1	0.01							1.3	3.08	0.002[d]	2.0[c]	3.22	0.002[d]	2.1	4.59	0.002[d]	0.6	10

[a] $R_P = 100\sum(k^3\chi_{exp} - k^3\chi_{theory})^2/\sum(k^3\chi_{exp})^2$. [b] CN of second shell O was correlated (set equal) to CN of second shell C. [c] CN of second shell C bound to S was correlated (set equal) to CN of first shell S. [d] Debye−Waller factors (σ^2) for second and higher atomic shells were fixed at 0.002. [e] A multiple three-legged scattering (Hg−S−C) was included in the fits with CN = 2, R (Å) = 3.54, σ^2 (Å^2) = 0.002 (MeHg−S resin), and CN = 4, R (Å) =3.64, σ^2 (Å^2) = 0.002 (Hg−S resin).

In the Hg/Org-S$_{RED}$ = 0.01 sample, the peak at ~2.7 Å (2.3−3.0 Å) reflects a second shell contribution best fitted by a mixture of 1.3 S at 3.08 Å and 2.0 C at 3.22 Å. Note that the CN of second shell C was fixed to be equal to the CN of first shell S. This is justified by the fact that, for every thiol group involved in the bonding, one carbon atom should be observed in the second shell. An inclusion of second shell S resulted in a 15% improvement of the fit, as compared with a second shell of only C backscatters (also if a short Hg---C distance was considered). Inclusion of O/N atoms in the second shell lowered the goodness of fit significantly. A second shell O/N contribution was only possible if the E_0 was shifted 10 eV, resulting in a breakdown of the first shell fit. This was true for both raw data and back-filtered data of the second shell peak. This is strong evidence that carboxyl and amino groups that may be situated adjacent to thiol groups, such as in the amino acids cysteine and glutathione, are not involved in the complexation. EXAFS data on Hg−cysteine complexes show no sign of involvement of amino or carboxyl groups (*35*). For the Hg/Org-S$_{RED}$ = 0.05 sample, a model with 0.5 S at 2.95 Å and 1.2 C at 3.42 Å in the second shell gave the best fit to data. The second shell S improved the fit by approximately 20%, as compared to a model assuming only involvement of thiols with C atoms at 3.2−3.4 Å.

The significant second shell S contribution at 2.95−3.08 Å in the Hg/Org-S$_{RED}$ = 0.01 and Hg/Org-S$_{RED}$ = 0.05 samples is a strong indication for involvement of a distant S in a weaker attraction. This could be a third thiol, but is more likely S groups such as disulfides (RSSR), sulfides (RSR), or polysulfides (RSS$_n$R) that are known to form weak intermolecular attractions with Hg. Klemens et al. (*24*) reported a second shell Hg---S interaction at 2.96−3.09 Å with methionine, in connection with a first shell Hg−thiol bond of 2.32−2.38 Å for plastocyanin, azurin, laccase, and stellacyanin. Similarly, Church et al. (*36*), in crystallographic determinations of plastocyanin−Hg complexes, found a short interaction at 2.38 Å with thiol S and a longer interaction with methionine S at 3.02 Å. The finding is also in agreement with one of the two possible models presented by Xia et al. (*11*) for Hg complexed by humic substances, with a second shell contribution from S at 2.93 Å. The second shell Hg---C distance of 3.22−3.42 Å is in fair agreement with a reported range of 3.20−3.35 Å for Hg−SR associations (Table S1, Supporting Information), as well as with data obtained for our MeHg−SR and Hg−SR model compounds (Table 2). A proposed structure for the complexation of Hg in the Hg/Org-S$_{RED}$ = 0.01−0.05 samples is illustrated in Figure 3a. This structure is in agreement with EXAFS studies of cysteine (*35*), at ratios of H_2Cys/Hg < 2.2, and is justified by the high thermodynamic stability of linear S−Hg−S configurations (log K_1 = 42−44) over combinations of one thiol and one amino acid or carboxyl group (log K_1 = 35−38) (*37*).

For the organic soil samples with addition of 1.2 mg of Hg g^{-1} or more (Hg/Org-S$_{RED}$ = 0.10−0.33), O/N ligands were increasingly involved in the complexation, resulting in a mixture of O/N and S binding sites. This is expected when high-affinity reduced S sites get saturated, and is reflected in the RSF by a broadening and shift of the first major peak to lower angstroms (Figure S2, Supporting Information). The reduced S contributions in samples with Hg/Org-S$_{RED}$ = 0.10−0.33 showed a second shell Hg---C (−S) distance of 3.29−3.33 Å, well in agreement with the Hg−SR resin (Table 2). Not surprisingly, the increasing heterogeneity of binding ligands with increasing Hg concentrations resulted in a decreasing contribution from the four-legged MS at 4.6 Å. The change from pure S (in samples with Hg/Org-S$_{RED}$ < 0.10) to a mixture of S and O/N coordination at higher Hg loading was also clearly reflected in the first derivatives of the absorption edge of organic soil samples and model compounds (Figure S3, Supporting Information).

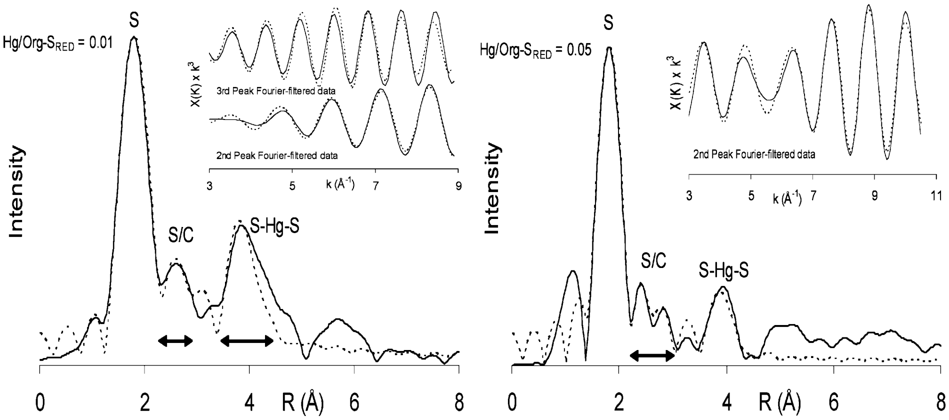

FIGURE 2. Radial structure functions for experimental data (solid lines) and fits (dotted lines) for the organic soil with addition of 0.1 mg of Hg g^{-1} (Hg/Org-S$_{RED}$ ratio = 0.01) and 0.6 mg of Hg g^{-1} (Hg/Org-S$_{RED}$ ratio = 0.05). The inserts show the back transforms (solid lines) and fits (dotted lines) of the S/C peak (second peak, first double arrow) and the S−Hg−S multiple scattering peak (third peak, second double-arrow), for the sample Hg/Org-S$_{RED}$ ratio = 0.01, and the S/C peak for the sample Hg/Org-S$_{RED}$ ratio = 0.05. Data are not corrected for phase shift.

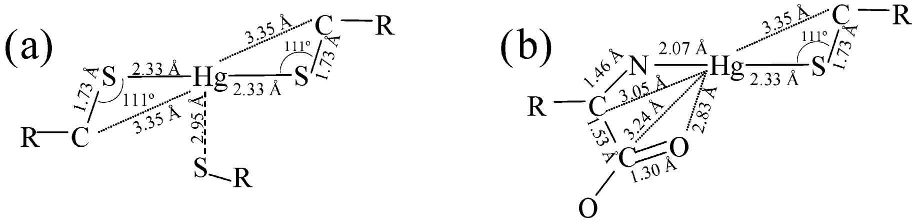

FIGURE 3. Proposed average structures for Hg complexed by organic soil at Hg/Org-S$_{RED}$ = 0.01 − 0.05 (a) and organic soil and HA at Hg/Org-S$_{RED}$ = 0.10 − 0.40 (b). Note that distances and angles in these structures reflect an average composition of the associations in organic soil and HA samples and that the true complexes may or may not be mixtures of different ligations. The N atom represents either an amino-N or a carbonyl-O group.

The contribution from O/N atoms in the first shell increased from 22 to 64% when the Hg addition was increased from 1.2 to 3.0 mg of Hg g^{-1} (Table 1). A further increase to 4.0 mg of Hg g^{-1}, however, lowered the contribution of O/N atoms to 56%. This apparent anomaly is explained by the quite large error in coordination numbers (±25%). The obtained Hg−O/N distance of 2.04−2.08 Å is in agreement with distances for two-coordinated Hg in well-defined organic molecules (Table S1, Supporting Information). An overlap in Hg−O and Hg−N bond distances makes it impossible to separate O and N using distances alone, even if first shell Hg−N distances on average are slightly longer (*38*).

If carboxyl groups are assumed to be involved in the complexation, one O atom and one C atom can be expected to occur within a distance of 2.60−2.83 Å for every carboxyl group (Table S1, Supporting Information). This was the case in the MeHg−OOCR model compound, even if the second shell Hg---C distance was slightly longer (Table 2). This relatively simple model, however, could not describe our soil data satisfactorily. A significantly better fit was obtained with two more distant C atoms for each second shell O atom, consistent with the structure illustrated in Figure 3b. This structure is in agreement with the complexation of methylmercury in α-amino acids such as DL-methionine (*39*), L-tyrosine (*30*), tryptophan (*33*), and glycine and L-alanine (*28*, *29*), in all cases involving an amino-N at 2.06−2.14 Å and a weaker attraction to a distant carboxyl-O at 2.67−2.82 Å.

Amino acids occur mainly as incorporated into organic macromolecules in soil, but concentrations of free molecules in solution may reach millimolar concentrations (*40*). Given that 38−56% of total N has been reported to be in the form of amino acids in peat soils (*41*), the total N of 18.3 mg g^{-1} in the organic soil could be assumed to reflect a Hg/amino-N molar ratio of 0.01−0.03 for the samples with a Hg/Org-S$_{RED}$ molar ratio of 0.10−0.33. If we speculate that as little as 10% of amino-N is represented by α-amino acids, a maximum of 30% of these groups would be saturated by Hg in the sample with Hg/Org-S$_{RED}$ = 0.33. Because O and N cannot be separated by EXAFS, also keto acids (carbonyl and carboxyl groups attached to the same carbon) are covered by the structure in Figure 3b. These functionalities also occur in organic soils (*40*). Recently reported EXAFS data suggest that Cu(II) is associated with amino acid and/or keto acid functionalities forming a five-membered chelate ring structure in the organic soil used in this study (*42*). This structure is similar to the structure in Figure 3b, but the ring is closed by a covalent bond formation with the carboxyl group. Our results are furthermore in agreement with the relative thermodynamic stability of thiol, α-amino acids, and carboxyl complexes. Smith et al. (*43*) compiled data from the literature and reported the average log K_1 value (at pH 7.0) for the formation of Hg−organic ligand complexes to decrease in the order thiol (16.1) > α-amino acid (7.3) > carboxyl acid (5.9).

The fact that the floating CN of first shell O/N and second shell O were of an equal size for all organic soil samples (Tables 1 and 2) gives additional support for a structure involving one amino/carbonyl (first shell O/N) and one carboxyl (second shell O) group. In order not to "over-parametrize" the model, only one second shell of C atoms were fitted at a distance of 3.10−3.14 Å. This distance is substantially longer than the distance of 2.6−2.9 Å, indicative for a first shell carboxyl-O and well in accordance with the average Hg---C distance that can be expected for a structure involving one amino/carbonyl and one carboxyl group. Furthermore, coordination numbers of 1.8, 1.5, and 1.3 for the second shell C in the organic soil samples with Hg/Org-S$_{RED}$ = 0.10−0.33 roughly correspond to 2 times the CN of first shell O/N atoms and 2 times the CN of second shell O atoms (Tables 1 and 2). This is in accordance with a model

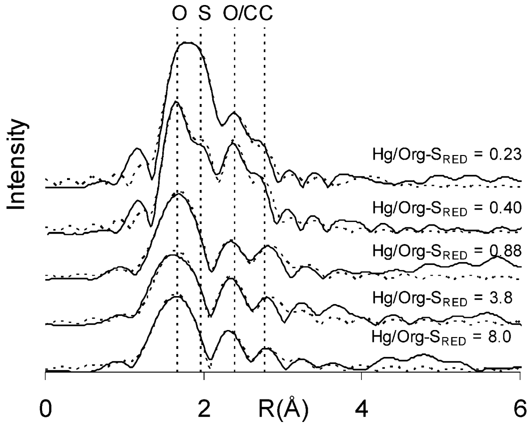

FIGURE 4. Fourier transformed EXAFS spectra (solid lines) and fits (dotted lines) for HA samples with addition of 3.2, 6.2, 14, 60 and 128 mg of Hg g^{-1}. Letters and vertical lines indicates first and second shell contributions from oxygen/nitrogen (O), sulfur (S), and carbon (C) atoms.

involving two O/N functional groups. A model involving only one carboxyl group (with one close and one more distant O) should result in CN values of 1:1:1 for first shell O, second shell O, and second shell C.

Humic Acids. Also for the HA samples, the first coordination shell is shifted to shorter distances with increasing Hg additions, reflecting an increasing relative contribution from O/N and decreasing relative contribution from S (Figure 4). The two HA samples with Hg/Org-S$_{RED}$ = 0.23−0.40 showed a slightly better signal-to-noise ratio than data for the organic soil samples with similar additions. This is reflected by the well-resolved features of the second coordination shell contributions in the RSF (Figure 4). These two samples were best fitted by a model including a mixture of S and O/N functional groups. The first shell Hg−S and second shell Hg---C(−S) distances were in agreement with data for the thiol resin model compounds, as well as with the organic soil (Tables 1 and 2). Also the first shell Hg−O/N and second shell Hg---C (−O/N) distances fell in the same range as those for the organic soil. The CN for second shell C(−O/N) corresponded to approximately 2 times the CN of first shell O/N and 2 times the CN of second shell O, giving support for a structure similar to Figure 3b. In line with this, the second shell Hg---C distance was too long to support a model involving only carboxyl groups (cf. Table S1, Supporting Information). In humic acids the concentration of amino acid nitrogen has been shown to be in the range 20−45% of total N (39). Thus, similar to the organic soil, concentrations of thiol and α-amino acid groups should be more than enough to complex all added Hg in the HA sample with Hg/Org-S$_{RED}$ = 0.23−0.40. In the three HA samples with the highest concentrations of Hg (Hg/Org-S$_{RED}$ = 0.88−8.0), only O/N functional groups could be detected in the first coordination shell. In the second shell, models with a Hg---C distance of 2.9 or 3.1−3.2 Å gave equal fits, suggesting that both monodentate complexation with carboxyl-O and a structure similar to the ring structure in Figure 3b are possible. Because of the relatively poor data quality and fits (cf. R_P values in Table 2), a more quantitative interpretation of the second shell was not made.

Concentration of High-Affinity Reduced S Sites in NOM. Determined coordination numbers for O/N and S in the first coordination shell can be used to calculate the proportion of reduced organic S atoms that take part in the complexation of Hg, using the following equation: $100[CN_S/(CN_S + CN_{O/N})][2(\text{Hg/Org-S}_{RED})]$. The factor 2 is due to the divalent charge of the Hg^{2+} ion. For the three organic soil samples, in which both S and O/N containing sites contributed to the complexation, on average 20% of the reduced organic S was calculated to be high-affinity sites (Table S3, Supporting Information). This can be compared with an average 29% when MeHg was used as a high-affinity S probe for the same organic soil as used in this study (*15*). Interestingly enough, the HA from Minnesota wetland showed a similar proportion of high-affinity S sites with an average of 29% for the two samples with lowest additions of Hg. Thus, based on Hg and MeHg EXAFS data, we conclude that approximately 20−30% of the reduced S, as determined by sulfur XANES, is represented by high-affinity sites for soft B-type metals. These high-affinity S groups likely are thiols. The rest of the reduced organic S are sulfides (RSR), disulfides (RSSR), polysulfides (RSS$_n$R), and possibly thiophenes. As shown in this study, some of these groups, likely situated close to thiols, may contribute to Hg complexation by more distant weaker bonds. Because a linear S−Hg−S coordination was determined at an Hg/Org-S$_{RED}$ molar ratio of 0.01, it is reasonable to assume that Hg^{2+} is complexed in a similar way in soils and waters with much lower Hg/Org-S$_{RED}$ molar ratios. These findings are important for further in-depth research of the biogeochemistry of Hg and MeHg, as well as in the selection of relevant complexation constants for Hg associations to NOM to be included in biogeochemical models.

Acknowledgments

We are grateful to Pierre-Emmanuel Petit and staff at ESRF beamline ID 26 and the staff at NSLS beamline X10C. We also thank Wolfgang Frech for assistance during sample preparation and data collection at ESRF. This study was funded by Swedish Research Council Contract No. 621-2001-1812.

Supporting Information Available

Description of the standard procedure for EXAFS data reduction, RSF data, and fits for model compounds (Figure S1a and S1b), RSF data and fits for organic soils with Hg/Org-S$_{RED}$ = 0.10−0.33 (Figure S2), normalized first derivatives for the XANES region (Figure S3a and S3b), bond distances and angles for well-defined Hg−S, Hg−N, and Hg−O associations in organic molecules (Table S1), calculations of degrees of freedom (Table S2), and calculations of the concentration of high-affinity S sites (Table S3). This material is available free of charge via the Internet at http://pubs.acs.org.

Literature Cited

(1) St. Louis, V. L.; Rudd, J. W. M.; Kelly, C. A.; Beaty, K. G.; Flett, R. J.; Roulet, N. T. Production and loss of methylmercury and loss of total mercury from boreal forest catchments containing different types of wetlands. *Environ. Sci. Technol.* **1996**, *30*, 2719−2729.

(2) Skyllberg, U.; Qian, J.; Frech, W.; Xia, K.; Bleam, W. F. Distribution of mercury, methyl mercury and organic sulphur species in soil, soil solution and stream of a boreal forest catchment. *Biogeochemistry* **2003**, *64*, 53−76.

(3) Watras, C. J.; Morrison, K. A.; Kent, A.; Price, N.; Regnell, O.; Eckley, C.; Hintelmann, H.; Hubacher, T. Sources of methylmercury to a wetland-dominated lake in northern Wisconsin. *Environ. Sci. Technol.* **2005**, *39*, 4747−4758.

(4) Downs, S. G.; Macleaod, C. L.; Lester, J. N. Mercury in precipitation and its relation to bioaccumulation in fish: A literature review. *Water Air Soil Pollut.* **1998**, *108*, 149−187.

(5) Benoit, J. M.; Gilmour, C. C.; Heyes, A.; Mason, R. P.; Miller, C. L. Geochemical and biological controls over methylmercury production and degradation in aquatic ecosystems. *ACS Symp. Ser.* **2003**, *835*, 262−297.

(6) Barkay, T.; Gillman, M.; Turner, R. R. Effects of dissolved organic carbon and salinity on bioavailability of mercury. *Appl. Environ. Microbiol.* **1997**, *63*, 4267−4271.

(7) Benoit, J. M.; Gilmour, C. C.; Mason, R. P. The influence of sulfide on solid-phase mercury bioavailability for methylation

by pure cultures of *Desulfobulbus propionicus* (1pr3). *Environ. Sci. Technol.* **2001**, *35*, 127−132.

(8) Skyllberg, U.; Xia, K.; Bloom, P. R.; Nater, E. A.; Bleam, W. F. Binding of mercury (II) to reduced sulfur in soil organic matter along upland-peat soil transects. *J. Environ. Qual.* **2000**, *29*, 855−865.

(9) Han, S.; Gill, G. A. Determination of mercury complexation in coastal and estuarine waters using competitive ligand exchange method. *Environ. Sci. Technol.* **2005**, *39*, 6607−6615.

(10) Khwaja, A. R.; Bloom, P. R.; Brezonik, P. L. Binding constants of divalent mercury (Hg^{2+}) in soil humic acids and soil organic matter. *Environ. Sci. Technol.* **2006**, *40*, 844−849.

(11) Xia, K.; Skyllberg, U. L.; Bleam, W. F.; Bloom, P. R.; Nater, E. A.; Helmke, P. A. X-ray absorption spectroscopic evidence for the complexation of Hg(II) by reduced sulfur in soil humic substances. *Environ. Sci. Technol.* **1999**, *33*, 257−261.

(12) Hesterberg, D.; Chou, J. W.; Hutchison, K. J.; Sayers, D. E. Bonding of Hg(II) to reduced organic sulfur in humic acid as affected by S/Hg ratio. *Environ. Sci. Technol.* **2001**, *35*, 2741−2745.

(13) Swift, R. S. Organic matter characterization. In *Methods of soil analysis. Part 3. Chemical methods*; Sparks, D. L., Ed.; Soil Science Society of America Book Series 5; SSSA: Madison, WI, 1996; pp 1018−1020.

(14) Xia, K.; Weeser, F.; Bleam, W. F.; Bloom, P. R.; Skyllberg, U. L.; Helmke, P. A. XANES studies of oxidation states of sulfur in aquatic and soil humic substances. *Soil Sci. Soc. Am. J.* **1998**, *62*, 1240−1246.

(15) Qian, J.; Skyllberg, U.; Frech, W.; Bleam, W. F.; Bloom, P. R.; Petit, P.-E. Bonding of methyl mercury to reduced sulfur groups in soil and stream organic matter as determined by X-ray absorption spectroscopy and binding affinity studies. *Geochim. Cosmochim. Acta* **2002**, *66*, 3873−3885.

(16) Lytle, F. W.; Greegor, R. B.; Sandstrom, D. R.; Marques, E. C.; Wong, J.; Spiro, C. L.; Huffman, G. P.; Huggins, F. E. Measurement of soft X-ray absorption spectra with a fluorescent ion chamber detector. *Nucl. Instrum. Methods Phys. Res.* **1984**, *226*, 542−548.

(17) Ressler, T. WinXAS: a program for X-ray absorption spectroscopy data analysis under MS-Windows. *J. Synchrotron Radiat.* **1998**, *5*, 118−122.

(18) Rehr, J. J.; Booth, C. H.; Bridges, F.; Zabinsky, S. I. X-ray-absorption fine structure in embedded atoms. *Phys. Rev. B* **1994**, *49*, 12347−12350.

(19) Zabinsky, S. I.; Rehr, J. J.; Ankudinov, A.; Albers, R. C.; Eller, M. J. Multiple scattering calculations of X-ray absorption spectra. *Phys. Rev. B* **1995**, *52*, 2995−3009.

(20) Yoon, S.-J.; Diener, L.; Bloom, P. R.; Nater, E. A.; Bleam, W. F. X-ray absorption studies of CH_3Hg^+-binding sites in humic substances. *Geochim. Cosmochim. Acta* **2005**, *69*, 1111−1121.

(21) Yamamura, T.; Watanabe, T.; Kikuchi, A.; Yamane, T.; Ushiyama, M.; Hirota, H. Conformation control of peptides by metal ions. Coordination, conformation correlation observed in a model for Cys-X-Y-Cys/M^{2+} in proteins. *Inorg. Chem.* **1997**, *36*, 4849−4859.

(22) Bramlett, M. J.; Im, H.-J.; Yu, X.-H.; Chen, T.; Cai, H.; Roecker, L. E.; Barnes, C. E.; Dai, S.; Xue, Z.-L. Reactions of thioether carboxylic acids with mercury(II). Formation and X-ray crystal structure of mercury(II) mercaptoacetate. *Inorg. Chim. Acta* **2004**, *357*, 243−249.

(23) Ueyama, N.; Taniuchi, K.; Okamura, T.-A.; Nakamura, A.; Maeda, H.; Emura, S. Effect of the NH---S Hydrogen bond on the nature of Hg-S bonding in bis[2-(acylamino)benzenethiolato]mercury-(II) and bis[2,6-bis(acylamino)benzenethiolato]mercury(II) complexes. *Inorg. Chem.* **1996**, *35*, 1945−1951.

(24) Klemens, A. S.; McMillin, D. R.; Tsang, H.-T.; Penner-Hahn, J. E. Structural characterization of mercury-substituted copper proteins. Results from X-ray absorption spectroscopy. *J. Am. Chem. Soc.* **1989**, *111*, 6398−6402.

(25) Leung, T. Y. B.; Gerstenberg, M. C.; Lavrich, D. J.; Scoles, G. 1,6-Hexanedithiol monolayers on Au(111): A multitechnique structural study. *Langmuir* **2000**, *16*, 549−561.

(26) Steudel, R. The chemistry of organic polysulfanes R-S_n-R ($n>2$). *Chem. Rev.* **2002**, *102*, 3905−3945.

(27) Alex, S.; Savoie, R.; Corbeil, M.-C.; Beauchamp, A. L. Complexation of glycylglycine by the methylmercury cation: vibrational spectroscopy and X-ray diffraction study. *Can. J. Chem.* **1986**, *64*, 148−157.

(28) Corbeil, M.-C.; Beauchamp, A. L. Crystal structure and vibrational spectra of the methylmercury complex with L-alanine. *J. Crystallogr. Spectrosc. Res.* **1989**, *19*, 123−134.

(29) Corbeil, M.-C.; Beauchamp, A. L.; Alex, S.; Savoie, R. Interaction of the methylmercury cation with glycine and alanine: a vibrational and X-ray diffraction study. *Can. J. Chem.* **1986**, *64*, 1876−1884.

(30) Alcock, N. W.; Lampe, P. A.; Moore, P. Crystal structures of methyl(L-tyrsinato)mercury(II) monohydrate and [L-(2-amino-4-phenylbutanoato)]methylmercury(II). *J. Chem. Soc., Dalton Trans.* **1978**, *13*, 1324−1328.

(31) Bowmaker, G. A.; Churakov, A. V.; Harris, R. K.; Oh, S.-W. Vibrational spectroscopy and solid-state MAS NMR studies of mercury(II) acetate complexes [Hg(X)OAc] crystal structure of [Hg(CN)OAc]. *J. Organomet. Chem.* **1998**, *550*, 89−99.

(32) Forniés, J.; Martín, A.; Sicilia, V.; Villarroya, P. Reactivity of $[M(C{\wedge}P)(S_2CNMe_2)]$ [M=Pt, Pd; $C{\wedge}P=CH_2\text{-}C_6H_4\text{-}P(o\text{-tolyl})_2\text{-}\kappa C,P$] toward Mercury(II) carboxylates. X-ray molecular structures of $[Pt(C{\wedge}P)\text{-}S_2CNMe_2)(O_2CCF_3)Hg(O_2CCF_3)]$ and $[Pd(S_2CNMe_2)\text{-}\{\mu\text{-}P(o\text{-tolyl})_2\text{-}C_6H_4\text{-}CH_2\text{-}\}(\mu\text{-}O_2CCH_3)Hg(O_2CCH_3)]$. *Organometallics* **2000**, *19*, 1107−1114.

(33) Corbeil, M.-C.; Beauchamp, A. L. Methylmercury(II) complexes with tryptophan and its *N*-acetyl derivative. *Can. J. Chem.* **1988**, *66*, 2458−2464.

(34) Barone, V.; Benchini, A.; Federico, I.; Uytterhoeven, M. G. Theoretical study of the electronic structure and of the mercury-carbon bonding of methylmercury(II) compounds. *J. Phys. Chem.* **1995**, *99*, 12743−12750.

(35) Jalilehvand, F.; Leung, B. O.; Izadifard, M.; Damian, E. Mercury-(II) cysteine complexes in alkaline aqueous solution. *Inorg. Chem.* **2006**, *45*, 66−73.

(36) Church, W. B.; Guss, J. M.; Potter, J. J.; Freeman, H. C. The crystal structure of mercury-substituted polar plastocyanin at 1.9-Å resolution. *J. Biol. Chem.* **1986**, *261*, 234−237.

(37) Casas, J. S.; Jones, M. M. Mercury (II) complexes with sulfhydryl containing chelating agents: stability constant inconsistencies and their resolution. *J. Inorg. Nucl. Chem.* **1980**, *42*, 99−102.

(38) Holloway, C. E.; Melnik, M. Mercury organometallic compounds—classification and analysis of crystallographic and structural data. *J. Organomet. Chem.* **1995**, *495*, 1−31.

(39) Wong, Y.-S.; Carty, A. J.; Chieh, P. C. Crystal structure of (DL-methionato)methylmercury(II). *J. Chem. Soc., Dalton Trans.* **1977**, *12*, 1157−1160.

(40) Stevenson, F. J. *Humus chemistry*—Genesis, Composition, Reactions; John Wiley and Sons: New York, 1994.

(41) Sowden, F. J.; Morita, H.; Levesque, M. Organic nitrogen distribution in selected peats and peat fractions. *Can. J. Soil Sci.* **1978**, *58*, 237−249.

(42) Karlsson, T.; Persson, P.; Skyllberg, U. Complexation of copper-(II) in organic soils and in dissolved organic matter—EXAFS evidence for chelate ring structures. *Environ. Sci. Technol.* **2006**, *40*, 2623−2628.

(43) Smith, D. S.; Bell, R. A.; Kramer, J. R. Metal speciation in natural waters with emphasis on reduced sulfur groups as strong metal binding sites. *Comp. Biochem. Physiol., C* **2002**, *133*, 65−74.

Received for review January 10, 2006. Revised manuscript received April 13, 2006. Accepted April 24, 2006.

ES0600577